Too much, too young?

Altered corticolimbic axonal innervation and resting state functional connectivity suggests sex-dependent outcomes in a rat model of early life adversity

Jennifer A. Honeycutt[1], Camila Demaestri[1], Shayna Peterzell[1], Marisa M. Silveri[2], Xuezhu Cai[3], Praveen Kulkarni[3], Miles G. Cunningham[4], Craig F. Ferris[3], Heather C. Brenhouse[1,*]

[1] Developmental Neuropsychobiology Laboratory, Dept. of Psychology, Northeastern University. Boston, MA 02115
[2] Neurodevelopmental Laboratory on Addictions & Mental Health, McLean Hospital, Belmont, MA 02478; and Department of Psychiatry, Harvard Medical School, Boston, MA 02115
[3] Center for Translational Neuroimaging, Dept. of Psychology, Northeastern University, Boston, MA 02115
[4] Laboratory for Neural Reconstruction, Dept. of Psychiatry, McLean Hospital, Belmont, MA 02478
[*] *Correspondence*: H.Brenhouse@NEU.edu; 360 Huntington Ave NI125, Northeastern University, Boston, MA 02115

Abstract

Background: Adverse early experiences significantly alter behavioral and neural trajectories via aberrant brain maturation. Children with a history of early life stress (ELS) exhibit maladaptive behaviors and increased risk of mental illness later in life. Evidence in ELS-exposed humans identifies a role of atypical corticolimbic development; specifically, within amygdala-prefrontal cortex (PFC) circuits, and show precocially mature corticolimbic functional connectivity (FC). However, the neurobiological substrates of such ELS-driven developmental changes remain unknown. Here, we identify putative neurobiological changes to determine the timeline of developmental perturbations following ELS in rats.

Methods: Anterograde axonal tracing from basolateral amygdala (BLA) to pre- and infralimbic (PL, IL) PFC was quantified at postnatal days (PD)28, 38, and 48, along with anxiety-like behavior, in maternally separated (ELS) or control reared (CON) male and female rats. Resting state (rs)FC was assessed at PD28 and PD48 in a separate cohort.

Results: PD28 female ELS show early maturation of BLA-PFC innervation, with ELS-related changes in the male group not appearing until PD38. Female ELS show altered rsFC at PD28 and PD48, with only transient ELS-related changes seen in male PL. In female ELS, decreased anxiety-like behavior was associated with increased BLA-IL rsFC.

Conclusions: These data provide evidence that female rats may be more vulnerable to the effects of ELS via precocial BLA-PFC innervation, which likely drives altered corticolimbic rsFC. These data also show evidence that increased BLA-IL rsFC is associated with behavioral resiliency following ELS in female rats, providing mechanistic insight into the underlying etiology of adversity-induced vulnerability and resiliency.

Keywords: Maternal Separation, Early Life Adversity, Prefrontal Cortex, Basolateral Amygdala, Development, Anxiety

Introduction

Exposure to adversity very early in life is associated with deleterious biological, psychological, and behavioral consequences across the lifespan (Smyke et al., 2007; McEwan, 2008; Maccari et al., 2014; Callaghan & Tottenham, 2016; Hane & Fox, 2016; Krugers et al., 2017). Male and female offspring appear to be affected differently by early life stress (ELS), with female offspring more prone to develop disorders such as anxiety and depression (Hammen et al., 2000; Heim et al., 2008; Davis and Pfaff, 2014). Importantly, these sequelae often emerge later in childhood or adolescence, providing an opportunistic window for intervention before psychopathology takes hold. Thus, development of effective intervention strategies will require biological and developmental targets that are specific to individuals based on factors such as sex and timing of stress exposure (Lupien et al., 2009). Growing evidence suggests that ELS in humans leads to life-long changes in connectivity between limbic and cortical regions (Choi et al., 2009; Van Tieghem and Tottenham, 2018), with consequential deficits in emotion and cognition (Tyrka et al., 2013). Recent human imaging, as well as animal studies, highlight the importance of corticolimbic circuitry in the regulation of affective behavior and its disruption in mental disorders (Herringa et al., 2013, Bangasser and Valentino, 2014; Killgore et al., 2014), and highlight alterations directly related to ELS (Kaiser et al., 2018). Specifically, Tottenham and colleagues have illustrated that normative developmental changes in task-based functional connectivity (FC) between the amygdala and the medial prefrontal cortex (mPFC) are accelerated after ELS, with associated changes in anxiety (Gee et al., 2013), and is likely to be particularly evident in female offspring (Dickie and Armony, 2008). While amygdala-mPFC FC typically transitions in adolescence to enable efficient top-down emotional processing, children institutionalized during the first two years of life in orphanages display a *precocial* development of amygdala-mPFC FC. The anatomical substrates for this accelerated corticolimbic connectivity, however, remain unknown.

In the rat, the basolateral amygdala (BLA) sends glutamatergic inputs to the mPFC and modulates anxiety-related behaviors (Felix-Ortiz, 2016), the recall of emotionally salient information (McGaugh, 2004), decision-making (St Onge et al., 2012), and goal-directed behavior (Schoenbaum et al., 2000). Notably, two distinct subpopulations of BLA neurons have been found to project to different regions of the mPFC (Senn, 2014); projections to the dorsal (prelimbic; PL) region of the mPFC are active during threat-associated fear learning and expression, whereas projections from the BLA to the ventral (infralimbic; IL) region of the

mPFC are active upon extinction of fear learning, or learning about safety signals. In typically developing male rats, BLA innervation of the mPFC increases through adolescence (Cunningham et al., 2002), which likely contributes to the healthy maturation of threat and safety appraisal, though BLA-mPFC axonal innervation has not yet been evaluated in female model systems. Additionally, the effects of ELS on axonal sprouting from the BLA to the PL or IL have not yet been elucidated.

Surprisingly little (Herringa et al., 2013) is known about the interaction of sex and ELS on corticolimbic development, despite a striking sex difference in the clinical time-course and symptomology of ELS effects (Martin et al., 2014, Wainwright and Surtees, 2002). Notably, typically developing female offspring display earlier maturation of the PFC (Lenroot et al., 2007; Lenroot and Giedd, 2010). Identifying how ELS affects these sex-dependent trajectories is crucial to understanding sex differences in vulnerability and to develop individually-targeted intervention strategies. Therefore, here we used anterograde tracing to examine the effect of ELS on BLA-PFC innervation over development in male and female rats. We hypothesized that if heightened anxiety-like behaviors following ELS are associated with increased BLA-derived PFC innervation, then rats exposed to ELS via repeated pre-weaning maternal separation will display anxiety-like behavior and increased BLA-PFC innervation, and these effects will be more robust in the female group.

While task-based FC illustrates coordinated responsivity to anxiety-provoking stimuli (e.g., Gee et al., 2013), resting-state FC (rsFC) is an excellent metric for probing the functional integrity of the amygdala-PFC circuit independent of task demands (Alarcón et al., 2015; Gabard-Durnam et al., 2016; Thomason et al., 2011a; 2011b). Moreover, accumulating evidence shows that task-based neural activity and behavior can be predicted from individual rsFC differences in the corresponding neural circuit (e.g. Mennes et al., 2011). Effects of ELS on corticolimbic rsFC in humans are inconsistent, likely because of reliance on autobiographical questionnaires, different ages of measurement, and different criteria for ELS. While some studies report decreased rsFC in ELS-exposed individuals (e.g., Burghy et al., 2012, Fan et al., 2014), others report an early emergence of higher corticolimbic rsFC (Graham et al., 2015). In the rat, maternal separation results in the early emergence of adult-like fear learning based in fronto-amygdala circuitry (Callaghan and Richardson, 2011) and an early emergence of amygdala structural maturation (Ono et al., 2008). Early maturation of corticolimbic connectivity likely has deleterious consequences because a sufficient degree of PFC immaturity in the juvenile period is reportedly critical for learning anxiolytic cues (i.e., safety signals) in adulthood (Yang et al., 2012). Therefore, a back-translation is provided, in order to examine whether ELS-exposed rats display similarly accelerated maturation of amygdala-PFC FC to that of humans with a history of adversity, with increased BLA-PFC innervation as an anatomical substrate that drives sex-specific developmental effects.

Methods and Materials

Subjects

For Study 1 (BLA-mPFC innervation) and Study 2 (rsFC), timed-pregnant female Sprague-Dawley rats (Charles River, Wilmington, MA) arrived at our facility at gestational day 15. All rats were housed under standard laboratory conditions in a 12h light/dark cycle (lights on at 0700h), in a temperature- and humidity-controlled vivarium with access to food and water *ad libitum*. Following birth (designated as postnatal day [PD] 0), entire litters were randomly assigned as either: 1) control (CON), and left undisturbed with the exception of normal cage-changing twice/week and weighing procedures (weights taken at PD9, 11, 15, and 20); or 2) early life stress (ELS) via a maternal separation paradigm, as described previously (e.g., Grassi-Oliveira et al,, 2016; Ganguly et al., 2019) and outlined below. All pups were weaned at PD21 into same-sex mixed-litter pairs with free access to food and water and left undisturbed until needed for surgery/behavioral assessment for Study 1 at the appropriate ages (PD21/28, 31/38, or 41/48, respectively; see Figure 1A). Separate cohorts were used for Study 2, with all pups weaned at PD21 into same-sex mixed-litter pairs with free access to food and water and left undisturbed until needed for behavior and rsFC at the appropriate ages (PD28 and PD48). Study 2 subjects were imaged at both ages, with protocol described below. All experiments were performed in accordance with the 1996 Guide for the Care and Use of Laboratory Animals (NIH) and with approval from Northeastern University's Institutional Animal Care and Use Committee.

Maternal Separation Procedure

Whole litters were randomly assigned to CON or ELS groups at PD0, and only one rat per litter was assigned to each experimental group (i.e., age and sex) to avoid possible litter effects. On PD1 all litters were culled to 10 (+/-2) pups while maintaining an equal ratio of male and female offspring whenever possible. Pups assigned to ELS groups were separated from their dams and littermates in individual cups with home cage pine shavings within a circulating water bath (37°C) from PD2-PD10. At PD11-20, when body temperature is self-regulated, pups were individually separated into small cages. Separations lasted for 4 hours each day beginning at 0900h and, upon completion, pups were reunited with their dams and littermates and left undisturbed until the next day. During separations pups were deprived of maternal tactile stimulation and nursing, but not from maternal odor. ELS dams remained in their home cages but were deprived of their entire litters during separations.

Study 1: BLA-PFC Innervation

Surgeries

Male and female rats from CON and ELS litters at either age PD21, PD31, or PD41 underwent stereotaxic surgery to inject biotinylated dextran amine (BDA; 10,000MW anterograde neural tracer; Life Technologies NeuroTrace BDA 10000 Neuronal Tracer Kit; reconstituted with phosphate buffered saline (PBS) to obtain a final concentration of 10%) into the BLA (see Figure 1B for location coordinates). To ensure a maximal amount of tagging without excess bolus outside of the BLA, 200nL (0.2μl) of 10% BDA was injected into the BLA using a 32 gauge Neuros syringe (Hamilton Company) mounted to the stereotaxic apparatus, and attached to a remote microinfusion pump (11 Elite Nanomite Programmable Infusion Pump; Harvard Apparatus).

Rats were first anesthetized with Isoflurane in an induction chamber before beginning surgical procedures. The surgical site was shaved, and the animal was secured via ear bars, with top incisors positioned over a bite bar within a nose cone to provide continuous Isoflurane anesthetic maintenance during surgery. Each rat received a subcutaneous injection of Buprenex (buprenorphine; 0.03mg/kg body weight) as a postoperative analgesic. Once sufficiently anesthetized, measured via lack of pedal reflex, an incision was made in the skin along the midline of the skull to visualize Bregma and Lambda. Dorsal-ventral (DV) coordinates for Bregma and Lambda were taken to ensure that the skull was level, and Bregma was used as a landmark to navigate to the skull position directly above the BLA. A small burr hole was drilled into the right hemisphere of the skull based on these coordinates, and the needle was slowly lowered into the BLA (Figure 1B). DV depth was calculated from dura surface to account for individual differences in skull thickness. Once needle was lowered to the target, BDA was slowly infused at a rate of 40nL/min over the course of 5 minutes. The needle was then left in place for an additional 5 minutes to allow for diffusion of the BDA solution into the surrounding tissue before being slowly retracted. The incision was sutured, and rats were returned to individual cages and allowed 5-6 days

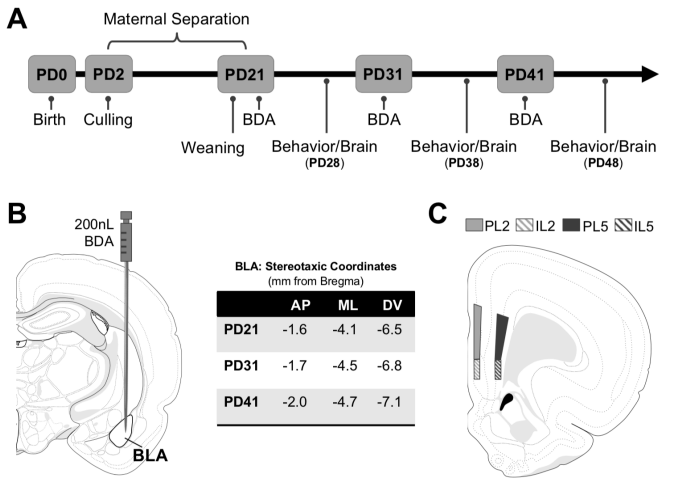

Figure 1. Timeline and methodology for study 1.
(**A**) Methodological timeline for Study 1 indicating maternal separation (for ELS groups) and weaning timeline. Biotinylated Dextran Amine (BDA) microinfusions were performed at PD21, PD31, or PD41. Behavior (EPM and OFT) were performed at PD28, PD38, or PD48. (**B**) Stereotaxic coordinates for surgeries at each developmental timepoint and map of basolateral amygdala (BLA) injection site where 200nL of BDA was infused. (**C**) Example of quantified regions of BLA-PFC axonal innervation. Quantification was conducted via unbiased stereology within the prelimbic (PL) and infralimbic (IL) in layers 2 and 5. Atlas modified from Swanson(2018). AP (anterior-posterior); ML (medial-lateral); DV (dorsal-ventral)

for recovery before behavioral testing, with all brain tissue collected one-week post-surgery.

Behavioral Assessment

Open Field Test

Open field (OFT) analysis was performed 6-7 days post-surgery. Animals were placed in an opaque Plexiglas open arena (100cm x 100cm) and monitored for 10 minutes by an overhead CCTV camera (Panasonic WV-CP500, Secaucus, NJ) attached to a computer equipped with Noldus Ethoviosion 9.0 software. Data was collected by an experimenter blind to condition and included: time spent in perimeter, time in center zone, number of center entries, and total distance traveled. The arena was cleaned with 50% ethanol solution between each animal.

Elevated Plus Maze

Elevated Plus Maze (EPM) performance was evaluated 6-7 days post-surgery in all animals and presentation of the EPM or OFT was counterbalanced to remove the possibility of artifacts based on order of testing. The apparatus was constructed of opaque Plexiglas with four radiating arms (50cm x 10cm) around a center square (10cm x 10cm), with 40cm-high walls surrounding two opposing arms, leaving the other two arms open. Between each animal 50% ethanol solution was used to clean the apparatus. Rats were acclimated to the testing room for 10min before testing began, and upon testing were placed in the center square of the apparatus under a red light facing a closed arm. Behavior was recorded for 5 minutes by an observer blind to group. Scoring of the following behaviors were performed: four-paw entries into/time spent (seconds) in open and closed arms, number of arm crossings, and head dips.

Tissue Collection and Preparation

7 days post-surgery, rats were deeply anesthetized with CO_2 and transcardially perfused with ice-cold physiological (0.9%) saline, followed by ice-cold 4% paraformaldehyde solution. Brains were extracted from the skull and stored in 4% paraformaldehyde solution for 1 week before being transferred to a 30% sucrose solution for 4 days for cryoprotection. All brains were sliced into 40µm serial sections on a freezing microtome (Leica), with serial sections placed in well plates filled with freezing solution for storage in a -20°C freezer. Sections taken for analysis included those encompassing PFC (+5.2mm through +2.5mm from Bregma) and BLA (-1.4mm through -3.6mm from Bregma) as outlined in Paxinos and Watson (1997). Serial sections were collected such that coronal sections within a single well were separated by approximately 240µm.

BLA-derived axonal innervation of the PFC, in addition to the injection bolus within the BLA for each animal, was visualized using diaminobenzidine (DAB) as indicated by the manufacturer (NeuroTrace BDA Kit, Life Technologies). One well for each animal was used for each brain region (PFC, BLA). Free-floating sections were initially washed 2x10min in PBS (7.4 pH) on an agitator before being transferred into Avidin solution (1:4000 in 0.3% PBS-T; Life Technologies NeuroTrace BDA Kit) overnight at 4°C on an agitator. Sections were then washed 3x5min in PBS and transferred into 0.05% DAB solution (Life Technologies NeuroTrace BDA kit) for 10 minutes to process the stain. Finally, sections were washed in PBS, mounted on glass slides, and coverslipped with DPX. Adjacent sections were randomly sampled from each experimental group (*n*'s=4/group) and stained with Cresyl Violet to determine average volume of the BLA based on age, sex, and condition. There were no significant differences based on sex or condition, thus volumes were collapsed across these to determine the average BLA volume per age (Supplemental Figure 1).

Bolus Verification in the BLA and Criteria for Inclusion

To determine the total volume of the BDA bolus within the BLA at the injection site, six DAB-stained sections containing BLA and BDA bolus were selected for analysis for each animal (inter-slice interval of 240um). Volumetric analysis was conducted in StereoInvestigator (MBF Bioscience, Wilmington, VT) using a Cavalieri probe to estimate total bolus volume. Different markers were used to identify regions of the bolus that fell within the BLA versus those that fell outside. The approximate percentage of the BLA filled with BDA tracer was calculated by dividing the volume of the bolus within the BLA by the average total BLA volume, specific to age, for each animal. Only subjects with a bolus filling greater than 60% of the average BLA volume (with no more than 15% of total bolus volume outside of the BLA) were included in analyses. See Figure 2 for details on bolus size and representative cases.

Quantification of PFC Axonal Innervation

Three sections of each brain containing the prefrontal cortex (both PL and IL regions between +4.0mm through +2.8mm from Bregma, with an inter-slice interval of 240um) were used for stereological analysis in StereoInvestigator. BLA-derived axon terminal fiber length was estimated via a hemispheric SpaceBalls Probe in 4 regions per section: PL layer 2 (PL2) and 5 (PL5), and IL layer 2 (IL2) and 5 (IL5); see Figure 1C. Axonal fibers that were in focus over the probe sphere outline (probe radius = 10µm) through the Z plane were identified at 60x oil immersion to determine an overall estimate of axon terminal length in the regions of interest (Gundersen and Jensen, 1987; Gundersen et al., 1999; Mouton et al., 2002).

Statistical analyses of neuroantatomical and behavioral data

To determine the effects of sex, rearing, and age on the estimated total length of BLA-derived axonal innervation of the PFC, three-way ANOVAs were conducted within each collapsed region (PL, IL), as well as within each layer (PL2, PL5, IL2, IL5). Follow-up two-way ANOVAs were conducted separately for male and female groups to determine sex-specific effects of age and rearing condition on innervation results. EPM and OFT performance was analyzed via separate two-way ANOVAs in male and female rats to determine the effect of age and rearing condition on behavioral measures. Significant main effects and/or interactions

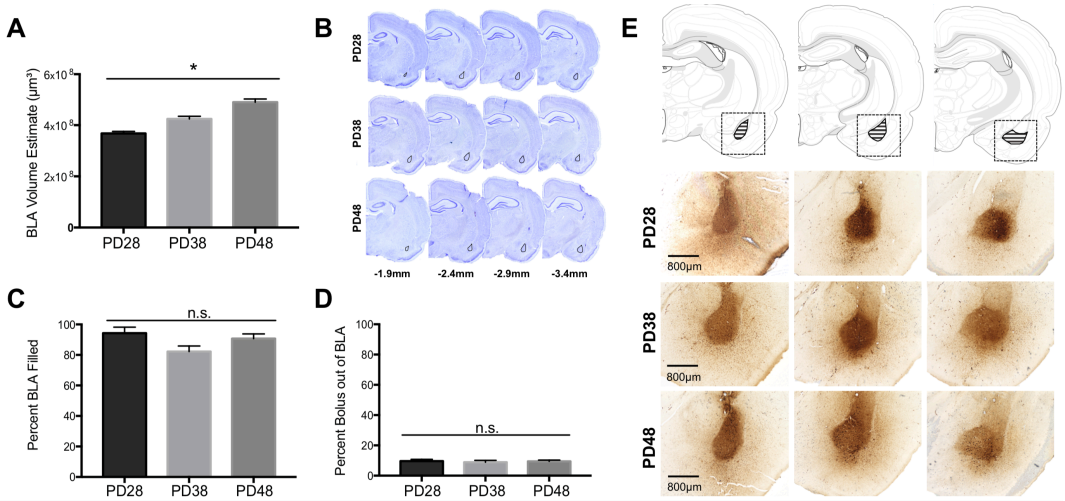

Figure 2. BLA volume and BDA anterograde tracer bolus sites.
The average volume of the BLA significantly increased with age (**A**) as quantified via Cresyl Violet staining of adjacent tissue sections (**B**), with coordinates below slices indicative of approximate distance (mm) from Bregma. There were no significant differences in the percent of BLA filled by the BDA anterograde tracer bolus between ages (**C**), nor was there any significant difference in the amount of bolus located outside of the BLA structure (**D**). Panel (**E**) shows representative photomicrographs of BDA bolus across the extent of the BLA for each age group examined. Atlas modified from Swanson (2018).
**p*<0.05; n.s. (non-significant)

were followed up where appropriate with Bonferroni post-hoc analyses and were corrected for multiple comparisons. Trending effects were followed up with post-hoc analyses only with moderate-to-strong effect sizes determined via partial eta squared analyses.

Separate linear regression analyses were conducted in male and female rats to determine whether there was a relationship between behavior in the EPM and/or OFT with axonal innervation into the PFC across age and rearing.

Study 2: Resting State Functional Connectivity (rsFC)

Imaging Protocol

MRI scanning was done in a Bruker BioSpec 7.0T/20cm USR horizontal magnet (Bruker, Billerica, MA) with a 20-G/cm magnetic field gradient insert (ID=12cm) capable of 120µs rise time. Rats were anesthetized with anesthesia maintained at 1-2% isoflurane and oxygen with a flow rate of 1 L/min throughout scanning, with breathing rate (40-50 breaths per minute) carefully monitored by an investigator and anesthetic levels adjusted accordingly when necessary. Rats were scanned at 300 MHz using a quadrature transmit/receive volume coil built into the rat head holder and restraint system (Animal Imaging Research, Holden, MA). Coil design provides coverage of the entirety of the brain from olfactory bulbs to brain stem with high B1 field homogeneity.

rsFC was acquired by gradient-echo triple-shot echo-planar imaging (EPI) pulse sequence with the following parameters: matrix size = 96x96x20; repetition time (TR)/echo time (TE) = 3000/15msec; voxel size = 0.312x0.312x1.2mm; slice thickness = 1mm; volume = 200. T2-weighted high-resolution anatomical scans were conducted using RARE pulse sequence with imaging parameters as follows: matrix size = 256x256x20; TR/TE = 4369/12msec; voxel size = 0.117x0.117x1mm; slice thickness = 1mm.

Data analyses were conducted using Analysis of Functional NeuroImages (AFNI_17.1.12; NIH), FMRIB software library (FSL, v5.0.9), and Advanced Normalization Tools (http://stnava.github.io/ANTs/). Resting-state Blood Oxygen-Level Dependent (BOLD) data were used for brain-tissue data extraction using 3Dslicer (https://www.slicer.org). Skull-stripped data were despiked to remove large signal fluctuations due to scanner and physiological artifacts during scanning. Slice-timing correction was conducted to correct the data from interleaved slice order data acquisition. Head motion correction was carried out using six parameters, using the first volume as the reference slice. Each subject was registered to a standard MRI Rat Brain Template (Ekam Solutions LLC, Boston, MA) using non-linear registration. In order to further reduce the effects from motion and physiological fluctuations, regressors comprised of six motion parameters, the average BOLD signal in white matter and ventricular regions, as well as motion outliers among all data volumes were fed into a nuisance regression model. Band-pass temporal filtering (0.01Hz-0.1Hz) and spatial smoothing (FWHM = 0.6mm) were performed on the residual data and followed by signal detrending.

Pre-Scan Elevated Plus Maze

Prior to imaging at PD28, all subjects were evaluated in the elevated plus maze to assess anxiety-like behavior to determine whether it could be predictive of alterations in rsFC. EPM methods were identical to those described for Study 1.

Statistical analysis of rsFC and behavioral data

rsFC was measured using a seed-based voxel-wise analysis, with the BLA as the seeded region of interest. The rsFC between the BLA and both the IL and PL regions of the mPFC specifically were the focus of the present study. Whole brain voxel-wise Pearson's correlation coefficients were calculated for each subject and were transformed for normality using Fisher's Z. A two-way mixed ANOVA (age as a within-subjects factor and stress as a between-subjects factor) was conducted for each sex using the AFNI 3dLME program, with a false discovery rate curve computed. Post-hoc contrast effects focusing on the effect of rearing condition (CON vs. ELS) at two levels of age (PD28 or PD48), as well as contrasts effects on the effect of age at two levels of rearing condition, were conducted where appropriate. Findings with a voxel-wise uncorrected *p* value of less than 0.005, with a minimal cluster size of more than 30 voxels, was regarded as statistically significant.

Linear regression analyses were conducted to determine the relationship between EPM performance and correlation coefficients of the BLA seeded rsFC data for both PL and IL in both males and females.

Results

Study 1: Neuroanatomy and Axonal Innervation

BLA volume:

A subset of tissue from each experimental group was analyzed for BLA volume with Cresyl Violet. The average BLA volume for each age (PD28, PD38, PD48) was calculated using the Cavalieri probe in StereoInvestigator (MBF Bioscience, Williston VT; *n*=16 per age group). To determine an effect of rearing or sex on BLA volume, a two-way ANOVA was conducted for each age, which revealed no significant effects of sex or rearing at any age (Supplemental Figure 1). Thus, results were pooled across sex and rearing to determine whether there was a change in BLA volume across development. A one-way ANOVA on these data

showed a main effect of age ($F_{2,48}$ = 31.74, p < 0.0001). Post-hoc Bonferroni analyses revealed a significant increase of BLA volume between PD28 and PD38 (p = 0.002), between PD28 and PD48 (p < 0.0001); and between PD38 and PD48 (p = 0.0002) (Figure 2A).

BLA Bolus:

The standard deviation of BLA volumes within each age only deviated approximately 1% from the mean volume, therefore the percent of BLA filled with BDA was calculated by dividing the volume of bolus within the BLA in each animal by the average BLA volume for each age. Additionally, the percent of bolus outside of the BLA was calculated for each animal by dividing the total bolus outside of the BLA by the total bolus volume counted.

Since age differences were detected in BLA volume, we examined whether there were differences in the amount of BLA filled as a function of age. A one-way ANOVA did not reveal an effect of percent of BLA filled by the bolus ($F_{2,88}$ = 3.030, p = 0.053) (Figure 2C). Furthermore, a one-way ANOVA analysis revealed no effect of percent of BDA bolus outside of the BLA across age groups ($F_{2,88}$ =0.133, p = 0.876) (Figure 2D). Representative BLA bolus can be seen in Figure 2E.

To ensure that the percentage of bolus within the BDA did not drive individual differences in axonal innervation of the PFC, linear regression analyses were used to calculate correlations between percent of filled BLA volume and total innervation in the PFC, as well as between the percent of BLA filled with tracer and total innervation in the PFC. These revealed no significant relationship between percent BLA filled and total innervation at any age (PD28: $R^2(28)$ = 0.064, p = 0.178; PD38: $R^2(27)$ = 0.004, p = 0.738; PD48: $R^2(30)$ = 0.057, p = 0.189). Additionally, linear regression analyses were used to investigate possible relationships between the total bolus volume (both within and outside of the BLA) and total PFC innervation, which revealed no significant correlation at any of the ages (PD28: $R^2(28)$ = 0.062, p = 0.185; PD38: $R^2(27)$ = 0.006, p = 0.696; PD48: $R^2(30)$ = 0.090, p = 0.096). See Supplementary Figure 2.

BLA-Derived Axonal Innervation:

There were no significant differences in probe volume or mounted thickness (all p's > 0.1) between groups based on age, sex, or rearing; thus, all analyses are presented as collected without corrections for counting probe volume or thickness (Supplemental Figure 3).

PL innervation:

A three-way ANOVA to determine the effects of rearing, sex, and/or age on axonal innervation into PL revealed a main effect of rearing ($F_{1,79}$ = 14.294, p < 0.0001) and a significant three-way interaction ($F_{2,79}$ = 5.244, p = 0.007) (Figure 3A). There was a trend toward a rearing x sex interaction ($F_{1,79}$ = 3.829, p = 0.054). A two-way ANOVA of male PL innervation showed a trend toward an age x rearing interaction ($F_{2,42}$ = 2.748, p = 0.076) with a moderate effect size (partial η^2 = 0.116) and follow-up post-hoc comparisons showed a significant ELS-driven increase in innervation at PD38 compared to CON (p = 0.031). Furthermore, a significant increase in innervation at PD38 compared to PD28 was observed in ELS (p = 0.044). Two-way ANOVA of female PL innervation showed a significant main effect of rearing ($F_{1,38}$ = 14.21, p < 0.001), with post-hoc comparison indicating significantly more PL innervation in ELS compared to female CON at PD28 (p = 0.009) and PD48 (p = 0.010). Representative photomicrographs are shown in Figure 4A.

Three-way ANOVAs to delineate layer-specific effects of innervation in PL revealed a significant main effect of rearing in PL2 ($F_{1,79}$ = 12.511, p = 0.001) and PL5 ($F_{1,79}$ = 12.925, p = 0.001). There were significant rearing x sex x age interactions in PL2 ($F_{2,79}$ = 4.655, p = 0.012) and PL5 ($F_{2,79}$ = 4.699, p = 0.012) (Figure 3B-C). In PL5, a significant rearing x sex interaction was observed ($F_{1,79}$ = 7.775, p = 0.007). Two-way ANOVAs were then conducted for each sex. In PL2, the male group showed a

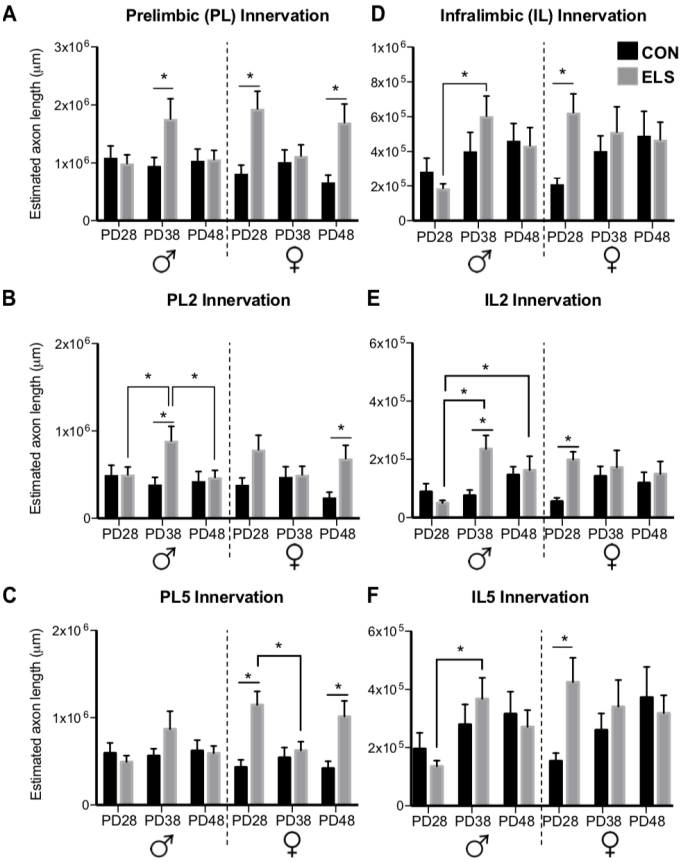

Figure 3. ELS leads to precocial BLA-PFC axonal innervation earlier in female than in male rats. BLA-PFC axonal innervation of anterogradely BDA-labeled fibers were quantified via unbiased stereology and are displayed here as an estimate of axon length (µm) in male and female rats in both PL (**A-C**) and IL (**D-F**). (**A**) shows total BLA-PL axonal innervation collapsed across layers, with innervation specific to layer 2 (L2; **B**) and layer 5 (L5; **C**) indicated in separate graphs. BLA axonal innervation quantification in the IL (**D**) is shown collapsed across all cortical layers. Specific innervation for L2 (**E**) and L5 (**F**) show comparably patterns of innervation. Data is presented as a function of sex (male, female), age at brain collection (PD28, PD38, PD48), and rearing condition (CON (black bars), ELS (grey bars)). *p < 0.05

significant main effect of rearing ($F_{1,41}$ = 4.365, p = 0.043) and a significant age x rearing interaction ($F_{2,41}$ = 3.236, p < 0.050), such that male ELS had more innervation than male CON only at PD38 (p = 0.007). Consequentially, male ELS displayed a significant increase in innervation at PD38 compared to PD28 (p = 0.049) and compared to PD48 (p = 0.030). A two-way ANOVA in female rats revealed a main effect of rearing ($F_{1,46}$ = 5.344, p = 0.025), such that the female ELS group had more PL2 innervation than the female CON group at PD48 (p = 0.047). Within PL5, the male group showed no significant effects or interactions (p's > 0.10). However, two-way ANOVAs of PL5 innervation in the female group revealed a significant main effect of rearing ($F_{1,38}$ = 17.760, p = 0.0001), as well as a trend toward a rearing x age interaction ($F_{2,38}$ = 2.987, p = 0.062). Post-hoc analyses revealed a significant effect of age in female PD28 compared to PD38 ELS groups (p = 0.041). Furthermore, a significant effect of rearing was found such that female ELS had more PL5 innervation than the CON female group at both P28 and P48 (p = 0.002 and 0.007, respectively).

IL Innervation:

A three-way ANOVA revealed no significant main effects or interactions (p's > 0.10) except for an observed trending effect of rearing ($F_{1,79}$ = 3.321, p = 0.072; Figure 3D). A two-way ANOVA in the male group showed a significant main effect of age ($F_{2,40}$ = 4.355, p = 0.019), which appeared to be driven by male ELS displaying increased IL innervation

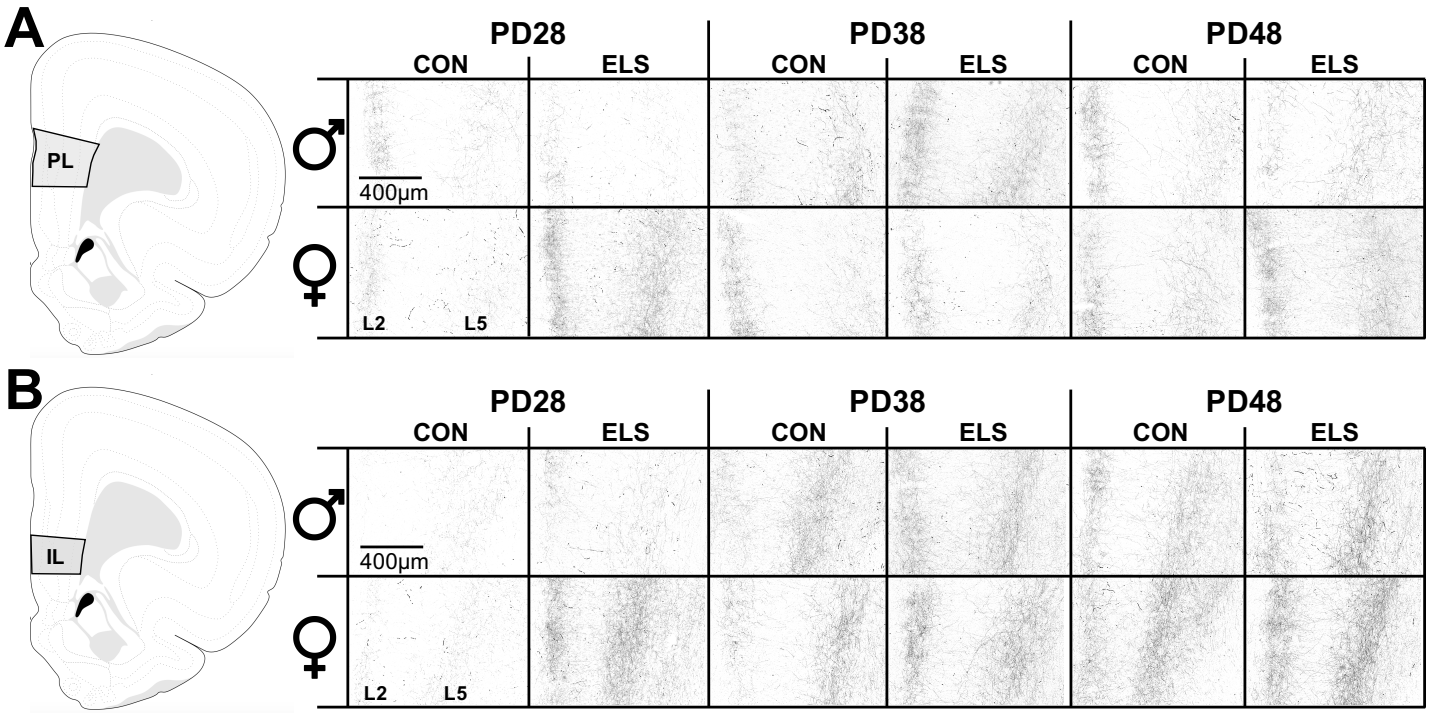

Figure 4. Both male and female rats show normative age-dependent increases in BLA-infralimbic (IL) axonal innervation; the female ELS group shows earlier IL innervation than the male group and CONs with transient ELS-driven influxes in PL in both sexes.
Estimated axon length in both the prelimbic (PL; **A**) and infralimbic (IL; **B**) cortices was quantified by amplifying the signal of anterogradely transported biotinylated dextran amine (BDA)-labeled axon fibers with diaminobenzidine (DAB) staining. Representative photomicrographs of both the PL (**A**) and IL (**B**) are depicted in the above panels, with dark axonal fibers clearly observed in layer 2 (L2; left side of each photomicrograph) and layer 5 (L5; right side of each photomicrograph). In the PL (**A**) there was consistent innervation across CON groups at all ages, with transient ELS-induced spikes of innervation occurring at PD28 and PD48 in female rats, and at PD38 in male rats. Within the IL (**B**), female rats showed precocial patterns of axonal innervation by PD28 that was comparable to adolescents and young adults, while male rats didn't show an ELS-driven increase in IL innervation until PD38. Photomicrographs were imaged at 10x mag. Atlas modified from Swanson (2018).

from PD28 to PD38 (p = 0.015). A two-way ANOVA in the female group showed no main effect of age or an age x rearing interaction. However, there was a trend toward a significant effect of rearing ($F_{1,38}$ = 3.627, p = 0.065), with a moderate effect size (partial η^2 = 0.087). Therefore, this was followed up with post-hoc indicating that the female ELS group had significantly more IL innervation than the female CON group at PD28 (p = 0.032; Figure 3D). Representative photomicrographs are presented in Figure 4B.

Three-way ANOVAs were conducted on both IL2 and IL5. In IL2, a main effect of rearing was evident ($F_{1,79}$ = 5.938, p = 0.017; Figure 3E), while in IL5 there were no significant main effects or interactions (p's > 0.10; Figure 3F). Two-way ANOVAs were conducted for each sex within each sub-region. The male group displayed a significant main effect of age ($F_{2,39}$ = 4.411, p = 0.019) in IL2, as well as a significant rearing x age interaction ($F_{2,39}$ = 4.521, p = 0.017). The male ELS group showed significantly more innervation into IL2 compared to the male CON group at PD38 (p = 0.007), but not at any other age (p's > 0.90). Developmentally, male ELS had significantly more innervation at PD38 compared to PD28 (p < 0.001), with a trend toward less innervation at PD48 compared to PD38 (p = 0.066). In the female group, there was a significant main effect of rearing ($F_{1,38}$ = 4.791, p = 0.035), driven by the fact that the female ELS group showed significantly more IL2 innervation than the female CON group at PD28 (p = 0.037; Figure 3E). A two-way ANOVA on IL5 male data showed a significant main effect of age ($F_{2,40}$ = 3.541, p = 0.038), with post-hoc comparisons revealing significantly more innervation in PD38 compared to PD28 in the ELS male group (p = 0.048). A two-way ANOVA on IL5 female data showed no significant main effects (p > 0.1). However, a trend toward a significant interaction effect ($F_{2,38}$ = 2.498, p = 0.096) with a moderate effect size (partial η^2 = 0.116) warranted follow up with post-hoc showing that the female ELS group had more IL5 innervation than the female CON group at PD28 (p = 0.044; Figure 3F).

EPM:

Two-way ANOVAs for each age revealed a main effect of rearing at PD28 ($F_{1,80}$ = 8.856, p = 0.004) and at PD38 ($F_{1,69}$ = 7.186, p = 0.009) with post hoc analysis showing the CON female group spent significantly more time in the open arms of the EPM than the ELS female group at PD28 (p = 0.049) and PD38 (p = 0.012) with no differences between the CON or ELS male groups at PD28 or PD38 (p > 0.40; Figure 5A-B). While no main effect of rearing was seen at PD48, two-way ANOVA did reveal a main effect of sex at PD48 ($F_{1,87}$ = 5.261, p = 0.024; Figure 5C).

To determine the impact of sex and rearing on the number of arm crossings and head dips in the EPM, a two-way ANOVA was performed for each age, revealing no significant main effects at PD28 or PD38 (p > 0.10) for arm crossings (Supplemental Figure 4A-B) or head dips (Supplemental figure 4D-E). At PD48, a main effect of sex was seen in number of crossings ($F_{1,87}$ = 19.320, p < 0.0001) and in number of head dips ($F_{1,87}$ = 8.754, p = 0.004) (Supplemental Figure 4C; 4F, respectively) showing a significantly higher number of crossings in female CON and ELS groups when compared to male CON and ELS groups (mCON v. fCON, p = 0.014; mCON v. fELS, p = 0.010; mELS v. fCON, p = 0.018; and mELS v. fELS, p = 0.012) and a higher frequency of head dips in the female compared to male CON (p = 0.028).

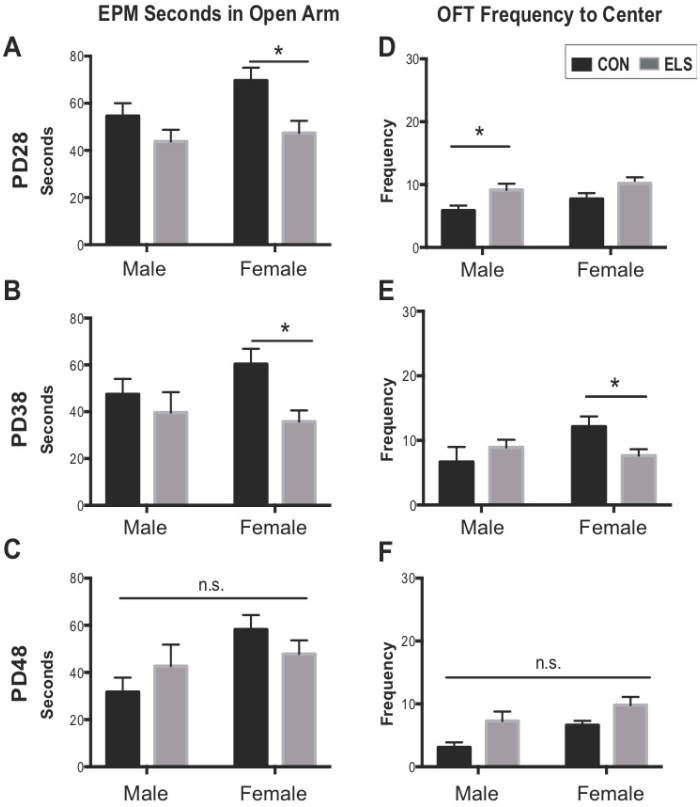

Figure 5. Anxiety-like behaviors following ELS are sex- and age-specific.
Anxiety-like behavior was assessed in the EPM and the OFT in both male and female CON (black bars) and ELS (grey bars) groups. Anxiety-like behavior in the EPM was determined via time spent in open arms (seconds; **A-C**). In the OFT, frequency to center entries was assessed across age (**D-F**). Females, but not males, showed more anxiety in the EPM in ELS groups at PD28 (**A**) and PD38 (**B**). Males showed less anxiety following ELS at PD28 (**D**). Females showed increased anxiety at PD38 in the OFT following ELS (**E**). *$p < 0.05$; n.s. (non-significant); EPM (elevated plus maze); OFT (open field test)

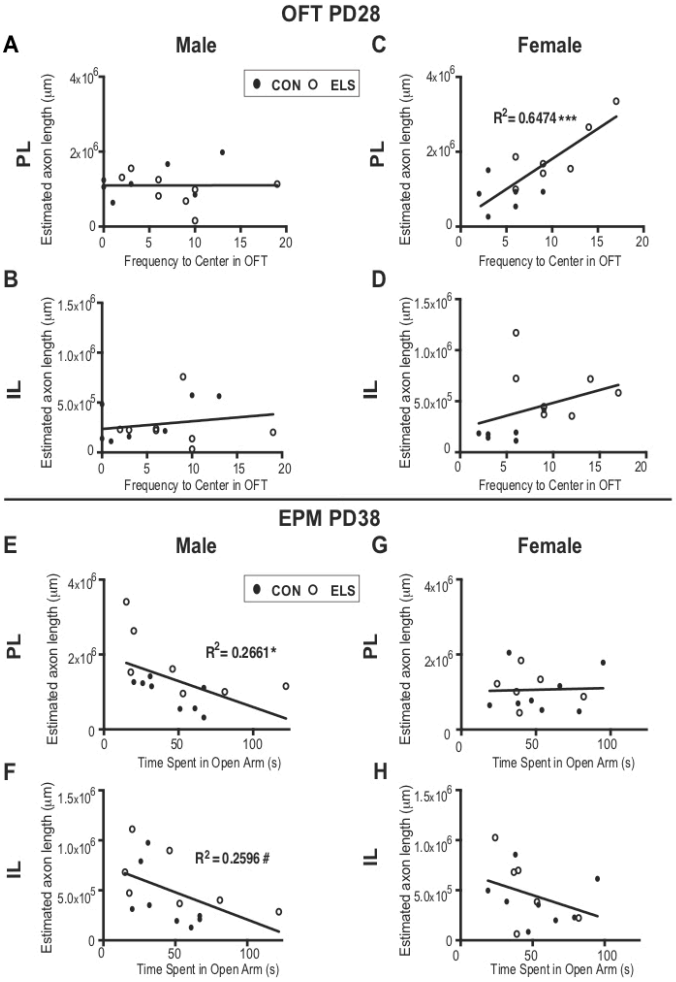

Figure 6. More mature BLA-PFC innervation is associated with decreased anxiety-like behavior in male and female rats and is dependent on age.
Results of linear regression analyses to determine the relationship between BLA-PFC axonal innervation (measured as an estimate of BDA-labeled axon fiber length) and performance in the OFT (**A-D**) and EPM (**E-H**). At PD28, female rats show decreased anxiety-like behavior in the OFT as a function of increased BLA innervation in the PL (**C**). Male rats also show decreased anxiety-like behavior as a function, though in the EPM of increased PL innervation, but not until PD38 (**E**), and also show a similar, though trending, effect in the IL (**F**). ***$p < 0.001$, *$p < 0.05$, #$p = 0.052$

OFT:

Two-way ANOVAs for each age revealed a significant main effect of rearing at PD28 for frequency of center entries in the OFT ($F_{1,73} = 9.367$, $p = 0.003$) with the CON male group entering the center fewer times than the ELS male group ($p = 0.046$; Figure 5D). A significant interaction between sex and rearing ($F_{1,50} = 5.587$, $p = 0.022$) was seen at PD38, with the CON female group entering the center more frequently than the ELS female group ($p = 0.043$; Figure 5E). At PD48, results indicated a main effect of sex ($F_{1,70} = 6.084$, $p = 0.016$) and rearing ($F_{1,70} = 9.018$, $p = 0.004$) (Figure 5F). There were no significant effects of sex or rearing on seconds spent in the center of the open field at PD28 or PD38. At P48, there was a significant main effect of sex ($F_{1,70} = 5.145$, $p = 0.026$) and of rearing ($F_{1,70} = 9.176$, $p = 0.003$). There were no significant effects of sex or rearing for distance traveled in the open field at PD28 or PD38; however, a main effect of sex was seen at PD48 ($F_{1,70} = 16.620$, $p = 0.0001$). Data for seconds spent in center and distance traveled can be seen in Supplemental Figure 5.

Relationships between innervation and behavior

At PD28, frequency to the center of the OFT arena did not correlate with innervation in the PL ($R^2(13) = 0.0399$, $p = 0.470$; Figure 6A) or in the IL ($R^2(13) = 0.00001$, $p = 0.990$; Figure 6B) in the male group. However, in the female group, higher frequency to the center of the OFT correlated with higher BLA innervation of the PL ($R^2(11) = 0.6474$, $p < 0.001$; Figure 6C), with no correlation in the IL ($R^2(11) = 0.1342$, $p = 0.218$; Figure 6D). Additionally, lower PL innervation at PD28 in the male group predicted more crossings in the EPM ($R^2(14) = 0.5120$, $p = 0.048$). At PD38, less time spent in the open arm of the EPM was associated with higher PL innervation in the male group ($R^2(13) = 0.2661$, $p = 0.049$), as well as at a trend level with higher IL innervation ($R^2(13) = 0.2596$, $p = 0.052$; Figure 6E-F). At PD38, seconds spent in the open arm of the EPM did not predict innervation in the PL ($R^2(12) = 0.0016$, $p = 0.893$) or in the IL ($R^2(12) = 0.1318$, $p = 0.202$; Figure 6G-H). No relationship between behavior and innervation was seen at PD48. Neither seconds spent in the OFT, nor distance traveled in the OFT predicted innervation in the PL or the IL at any ages (data not shown).

Study 2 Results: rsFC

Male Group

A 2-way ANOVA evaluating BLA-PL rsFC with age and rearing revealed no main effect of ELS, but a significant main effect of age ($F = 49.9$) and a significant interaction between age and rearing within two PL regions that met threshold criteria ($F = 15.8$; $F = 28.6$). Post-hoc comparisons showed a reduction in the strength of BLA-PL rsFC from PD28 to PD48 in both CON ($Z = -3.82$) and ELS ($Z = -3.26$) groups. There was no significant change in rsFC between CON and ELS at PD48; however, at

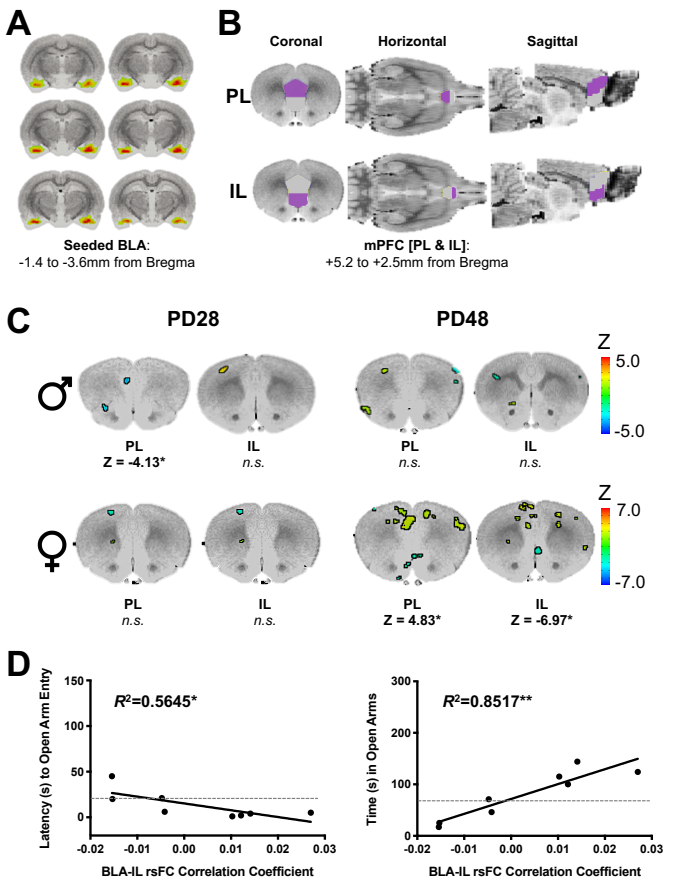

Figure 7. Effects of ELS on BLA-PFC functional connectivity are sex-specific and emerge in adolescence.

Resting state functional connectivity (rsFC) was assessed across development in male and female rats with a history of ELS or CON rearing with the basolateral amygdala (BLA) as the seeded region (**A**). The rsFC between the BLA and the mPFC – specifically the prelimbic (PL) and infralimbic (IL) cortices (**B**) – was assessed. (**C**) shows results from comparative analyses comparing CON and ELS groups at each age point (PD28 or PD48) in both male and female groups. Colored regions correspond to computed Z values and indicate specific regions within either the PL or IL that met criteria for significance with a minimum cluster size of 30 voxels. Generally, male rats show no group effects of ELS, with the exception of a finding of decreased BLA-PL rsFC in ELS compared to CON groups at PD28. Female rats showed no effect of ELS at PD28, but show striking differences in rsFC in both PL and IL at PD48. Decreased anxiety-like behavior, as assessed via time spent in open arms in the elevated plus maze (EPM) at PD28, was predictive of increased BLA-IL connectivity (**D**), suggesting that more functional connectivity between BLA and IL suppresses anxiety-like behavior in juvenility, but only in the female ELS group. $^{**}p < 0.005$, $^{*}p < 0.05$

PD28 CON showed stronger BLA-PL connectivity than ELS (Z = -4.13; Figure 7C). A similar 2-way ANOVA evaluating BLA-IL rsFC revealed a significant main effect of age (F = 49.9), with no significant post-hoc differences.

Female Group

A 2-way ANOVA (age x rearing) for BLA-PL revealed a main effect of age (F = 13.76) and rearing (F = 16.10), as well as a significant interaction (F = 12.65). Overall, BLA-PL rsFC decreased from PD28 to PD48 (Z = -3.6), while the ELS group displayed stronger connectivity compared to CON (Z = 3.5). Post-hoc showed no difference between CON and ELS at PD28, though showed a significant difference at PD48, when ELS had stronger BLA-PL connectivity than CON (Z = 4.83; Figure 7C). In comparing CON animals as a function of age, connectivity decreased from PD28 to PD48 (Z = -3.09). Conversely, in the ELS group BLA-PL connectivity increased from PD28 to PD48 (Z = 3.46).

The two-way ANOVA for BLA-IL rsFC showed no main effects of age or rearing, though a significant interaction was observed (F = 28.74). Overall, BLA-IL rsFC increased from PD28 to PD48 (Z = 3.35), and CON generally had weaker connectivity compared to ELS (Z = -3.79). Post-hoc tests revealed that, at PD48, ELS rats show less BLA-IL connectivity than CON (Z = -6.97; Figure 7C), and CON showed increased BLA-IL connectivity from PD28 to PD48 (Z = 4.47), with no significant change seen in ELS.

Relationship between rsFC and behavior

In the male group, rsFC correlation coefficients for both BLA-PL and BLA-IL did not correlate with PD28 EPM performance. In the female group, however, while PD28 EPM performance did not directly correlate with PD28 or PD48 rsFC in CON groups, performance did significantly correlate with BLA-IL correlation coefficients in the ELS female group tested at PD28. Specifically, higher/more positive correlation coefficients were associated with decreased latency to enter the open arm (R^2 = 0.5645, $p < 0.05$) and increased time spent in open arms (R^2 = 0.8517, $p < 0.005$). See Figure 7D.

Discussion

To our knowledge, this work is the first to describe the neuroanatomical etiology likely to underly pathological behavior and aberrant functional connectivity following ELS that has been observed in humans (e.g., Gee et al., 2013; Philip et al., 2013; Thomason et al., 2015; Teicher et al., 2016) and in animal models (Johnson et al., 2018). Here, we show significant sex- and age-dependent effects on BLA innervation in both PL and IL regions of the PFC following ELS in a rat model of caregiver deprivation. Our findings suggest that female offspring may be particularly vulnerable to neuroanatomical consequences of early adversity, with effects on innervation seen earlier in female offspring compared to a more protracted effect in male offspring. This is in line with human studies that have described sex-dependent effects of early adversity where female participants appear to exhibit more severe adolescent and later-life consequences, especially with regard to affective disorders (Humphreys et al., 2015).

The present findings indicate that BLA-mPFC innervation occurs in a protracted and bilaminar manner across development, with modest increases in both male and female CON rats at each developmental timepoint examined within the IL. Importantly, this clear developmental trajectory was seen in CON groups and supports previous developmental work in male rats (Cunningham et al., 2002), and extends it here by characterizing a similar trajectory in a cohort of female rats for the first time. While IL innervation shows a clear normative developmental increase, PL innervation seems to reach adult-like levels in both sexes earlier than was captured presently (Van Eden and Uylings, 1985; Bouwmeester et al., 2002). Following ELS, however, our data indicates that aberrant effects on innervation are apparent at PD28 in the female group, but not until PD38 in the male group, and this finding is conserved across both the PL and IL. However, while ELS conferred a similarly timed influx of BLA innervation in both regions, the long-term neuroanatomical alterations were different depending on region examined. Indeed, in the PL we see a transient effect of ELS that is age- and sex-dependent. In IL, however, there is evidence of precocial maturation, such that ELS induces BLA-IL innervation comparable to more mature (PD48) patterns in female juveniles (PD28) and male early adolescents (PD38). Importantly, this increased innervation in the juvenile female group is associated with decreased anxiety-like behavior in the OFT, while increased innervation in the male early adolescent group is associated with increased anxiety-like behavior in the EPM. This relationship supports previous work in ELS-exposed humans that suggest higher/more mature levels of BLA-PFC connectivity in juvenility is associated with compensatory decreases anxiety, with anxiety-like

behavior not emerging until adolescence/early adulthood (Callaghan and Tottenham, 2016).

Within the PL we observed that both male and female rats showed an unexpected transient spike in BLA-PL innervation that appeared to resolve at the following developmental timepoint. It is possible that reversal of the innervation seen at earlier timepoints may be due to pruning mechanisms in the PL (Koss et al., 2013) that typically occur in adolescence and may therefore mediate excess innervation (Rakic et al., 1994; Spear, 2000; Riccomagno and Klodkin, 2016). Prior work has shown a peak in BLA-PL connectivity, specifically at PD30 (Patwell et al., 2016), that may contribute to the present findings of transient ELS-exacerbated hyper-innervation. However, this does not explain why innervation spikes at PD28, is reduced to CON levels at PD38, and then returns to higher levels by PD48 in the female ELS groups. It is possible, however, that the temporary (one week) isolation following surgery may have acted as a secondary stressor acting in conjunction with pubertal changes to produce a resurgence of this earlier ELS-specific phenotype (Andersen and Teicher, 2008; Tzanoulinou and Sandi, 2016). Relatedly, the performance of surgery itself during peripubertal development compared to other time periods may have differentially interacted with ELS.

The results from the rsFC analyses revealed that the female group was selectively vulnerable to the effects of ELS on overall functional connectivity in both the PL and IL. Likely, this vulnerability is driven by early maturation of BLA-PFC innervation disrupting the functional relationship between these regions (Tottenham and Galván, 2016). Specifically, the female ELS group displayed dampened maturation of rsFC in the PL compared to the female CON group; while no effects of rearing were apparent at PD28, the female ELS group failed to display the decline in rsFC by PD48 that was observed in the female CON group. This is in line with previous work showing that BLA-mPFC connectivity is grossly unchanged at pre-weaning age following a limited bedding model (Guadagno et al., 2018), while rsFC later in life can be altered following ELS (Nephew et al., 2017). Maturation of BLA-IL rsFC was also disrupted by ELS, with no effect of rearing at PD28 but an age-related increase of connectivity at PD48 in female CON, but not the female ELS group. Interestingly, increased (i.e., more mature) rsFC BLA-IL connectivity in the female ELS group at PD28 was associated with decreased anxiety-like behavior at that age. This suggests that more mature connectivity in female juveniles may confer behavioral resilience, at least transiently as a compensatory measure, particularly since dampened connectivity has been associated with increased anxiety in adolescence (Kim et al., 2011; Nooner et al., 2013). Despite the male group showing similar (though more protracted) early innervation, it is possible that these more modest later changes may not yet translate to gross rsFC measures. However, it is also possible that such changes may have been subthreshold, as the innervation and behavioral correlations suggest that male rats with higher connectivity later exhibited more ELS-evoked anxiety.

The present findings support previous work indicating the distinct functional relationship between the BLA and PL and IL regions of the mPFC (Calhoon and Tye, 2015), with PL connectivity related to anxiogenic effects (Felix-Ortiz et al., 2016) and IL connectivity promoting anxiolytic effects on behavior (Maroun et al., 2012). Furthermore, these findings are in line with the idea that altered neuroanatomy and functionality of the PL and IL, along with the BLA, likely have reciprocal effects on one another, further contributing to exacerbation of ELS-induced anxiety-like phenotypes in adolescence and early adulthood (Likhtik and Paz, 2015; Zimmermann et al., 2019). While we are unable to directly link increased innervation patterns with alterations in functional connectivity here, evidence is provided suggesting that these changes are interrelated and likely underly ELS-induced pathology. It is possible that the early maturation of projections from the BLA into the PFC may overwhelm the slow-maturing reciprocal projections to the BLA that serve to dampen anxiety-related circuit activity in mature brains (Arruda-Carvalho et al., 2017; Selleck et al., 2018). Based on this evidence, it is proposed that increased BLA innervation of the PFC drives later life anxiety-like behavior and aberrant rsFC in female offspring, and likely underlies the sex-specific effects of ELS.

The present work systematically describes the developmental trajectory of BLA-PFC axonal innervation following ELS in both male and female rats. Furthermore, we provide evidence of a sex- and age-dependent effect of maternal separation-induced ELS on BLA-PFC rsFC. Furthermore, the innervation patterns – paired with the rsFC data – provide compelling evidence suggesting that ELS directly alters neuroanatomical development, and that these anatomical alterations likely lead to functional disturbances in key brain circuitry implicated in neuropsychiatric disorders. Taken together, it was observed that, in a rodent model, ELS disrupts normative development of both anatomical (axonal innervation) and functional (rsFC) connectivity within a circuit that regulates emotional processing, with female-specific effects and evidence of resilience in individuals with precocial maturation. These findings have implications for intervention based on experience, age, and sex – three functionally interactive factors that uniquely define risk in every individual.

Acknowledgements

The authors would like to sincerely thank Dr. Jens Foell (Florida State University) and Dr. Michael Rohan (McLean Hospital) for their feedback and suggestions for rsFC figures for this manuscript.

Funding

This work was funded by a grant from the NIMH (1R01MH107556-01) awarded to HCB.

Disclosures

CRF has a financial interest in Animal Imaging Research, the company that makes the rat imaging system. All other authors have no conflicts of interest to disclose.

References

Alarcón G, Cservenka A, Rudolph MD, Fair DA, Nagel BJ (2015). Developmental sex differences in resting state functional connectivity of amygdala sub-regions. Neuroimage 115: 235-244.

Andersen SL, Teicher MH (2008). Stress, sensitive periods and maturational events in adolescent depression. Trends Neurosci 31(4): 183-191.

Arruda-Carvalho M, Wu WC, Cummings KA, Clem RL (2017). Optogenetic examination of prefrontal-amygdala synaptic development. J Neurosci 37(11): 2976-2985.

Bangasser DA, Valentino RJ (2014). Sex differences in stress-related psychiatric disorders: neurobiological perspectives. Front Neuroendocrinol 35(3): 303-319.

Bouwmeester H, Wolterink G, Van Ree JM (2002). Neonatal development of projections from the basolateral amygdala to prefrontal, striatal, and thalamic structures in the rat. Journal of Comparartive Neurology 442(3): 239-249.

Burghy CA, Stodola DE, Ruttle PL, Molloy EK, Armstrong JM, Oler JA, Fox ME, Hayes AS, Kalin NH, Essex MJ, Davidson RJ, Birn RM (2012). Developmental pathways to amygdala-prefrontal function and internalizing symptoms in adolescence. Nat Neurosci 15(12): 1736-1741.

Calhoon GG, Tye KM (2015). Resilving the neural circuits of anxiety. Nat Neurosci 18(10): 1394-1404.

Callaghan BL, Richardson R (2011). Maternal separation results in early emergence of adult-like fear and extinction learning in infant rats. Behav Neurosci 125: 20-28.

Callaghan BL, Tottenham N (2016). The stress acceleration hypothesis: effects of early-life adversity on emotion circuits and behavior. Current Opinion in Behavioral Sciences 7: 76-81.

Choi J, Jeong B, Rohan ML, Polcari AM, Teicher MH (2009). Preliminary evidence for white matter tract abnormalities in young adults exposed to parental verbal abuse. *Biol Psychiatry* 65(3): 227-234

Cunningham MG, Bhattacharyya S, Benes FM (2002). Amygdalo-cortical sprouting continues into early adulthood: implications for the development of normal and abnormal function during adolescence. J Comp Neurol 453(2): 116-130.

Davis EP, Pfaff D (2014). Sexually dimorphic responses to early adversity: implications for affective problems and autism spectrum disorder. Psychoneuroendocrinology 49: 11-25.

Dickie EW, Armony JL (2008). Amygdala responses to unattended fearful faces: interaction between sex and trait anxiety. Psychiatry Research: Neuroimaging 162: 51-57.

Fan Y, Herrera-Melendez AL, Pestke K, Feeser M, Aust S, Otte C, Pruessner JC, Böker H, Bajbouj M, Grimm S (2014). Early life stress modulates amygdala-prefrontal functional connectivity: implications for oxytocin effects. Hum Brain Mapp 35(10): 5328-5339.

Felix-Ortiz AC, Burgos-Robles A, Bhagat ND, Leppla CA, Tye KM (2016). Bidirectional modulation of anxiety-related and social behaviors by amygdala projections to the medial prefrontal cortex. Neuroscience 321: 197-209.

Gabard-Durnam LJ, Gee DG, Goff B, Flannery J, Telzer E, Humphreys KL, Lumian DS, Fareri DS, Caldera C, Tottenham N (2016). Stimulus-elicited connectivity influences resting-state connectivity years later in human development: a prospective study. J Neurosci 36(17):4771-4781.

Ganguly P, Honeycutt JA, Rowe JR, Demaestri C, Brenhouse HC (2019). Effects of early life stress on cocaine conditioning and AMPA receptor composition are sex-specific and driven by TNF. Brain Behav Immun 78: 41-51.

Gee DG, Gabard-Durnam LJ, Flannery J, Goff B, Humphreys KL, Telzer EH, Hare TA, Bookheimer SY, Tottenham N (2013). Early developmental emergence of human amygdala-prefrontal connectivity after maternal deprivation. Proc Natl Acad Sci USA 110(39): 15638-15643.

Graham AM, Pfeifer JH, Fisher PA, Carpenter S, Fair DA (2015). Early life stress is associated with default system integrity and emotionality during infancy. J Child Psychol Psychiatry 56(11): 1212-1222.

Grassi-Oliveira R, Honeycutt JA, Holland FH, Ganguly P, Brenhouse HC (2016). Cognitive impairment effects of early life stress in adolescents can be predicted with early biomarkers: impacts of sex, experience, and cytokines. Psychoneuroendocrinology 71: 19-30.

Guadagno A, Kang MS, Devenyi GA, Mathieu AP, Rosa-Neto P, Chakravarty M, Walker DM (2018). Reduced resting-state functional connectivity of the basolateral amygdala to the medial prefrontal cortex in preweaning rats exposed to chronic early-life stress. Brain Structure and Function 223(8): 3711-3729.

Gundersen HJG, Jensen EB (1987). The efficiency of systematic sampling in stereology and its prediction. Journal of Microscopy 147(3): 229-263.

Gundersen HJG, Vedel Jensen EB, Kieu K, Nielsen J (1999). The efficiency of systematic sampling in stereology-reconsidered. Journal of Microscopy 193(3): 199-211.

Hammen C, Henry R, Daley SE (2000). Depression and sensitization to stressors among young women as a function of childhood adversity. Journal of Counseling and Clinical Psychology 68(5): 782-787.

Hane AA, Fox NA (2016). Early caregiving and human biobehavioral development: a comparative physiology approach. Current Opinion in Behavioral Sciences. 7: 82-90.

Heim C, Newport DJ, Mletzko T, Miller AH, Nemeroff CB (2008). The link between childhood trauma and depression: insights from HPA axis studies. Psychoneuroendocrinology 33(6): 693-710.

Herringa RJ, Birn RM, Ruttle PL, Burghy CA, Stodola DE, Davidson RJ, Essex MJ (2013). Childhood maltreatment is associated with altered fear circuitry and increased internalizing symptoms in late adolescence. *Proc Natl Aca Sci USA* 110(47): 19119-19124.

Humphreys KL, Gleason MM, Drury SS, Miron D, Nelson CA, Fox NA, Zeanah CH (2015). Effects of institutional rearing and foster care on psychopathology at age 12 years in Romania: follow-up of an open, randomized controlled trial. Lancet Psychiatry 2(7): 625-634.

Johnson FK, Delpech JC, Thompson GJ, Wei L, Hai J, Herman P, Hyder F, Kaffman A (2018). Amygdala hyper-connectivity in a mouse model of unpredictable early life stress. Translational Psychiatry 8: 49.

Kaiser RH, Clegg R, Goer F, Pechtel P, Beltzer M, Vitaliano G, Olson SP, Teicher MH, Pizzagalli DA (2018). Childhood stress, grown-up brain networks: corticolimbic correlates of threat-related early life stress and adult stress response. Psychol Med 48)7): 1157-1166.

Killgore WD, Britton JC, Schwab ZJ, Price LM, Weiner MR, Gold AL, Rosso IM, Simon NM, Pollack MH, Rauch SL (2014). Cortico-limbic responses to masked affective faces across ptsd, panic disorder, and specific phobia. Depress Anxiety 31(2): 150-159.

Kim MJ, Gee DG, Loucks RA, Davis FC Whalen PJ (2011). Anxiety dissociates dorsal and ventral medial prefrontal cortex functional connectivity with the amygdala at rest. Cereb Cortex 21(7): 1667-1673.

Koss WA, Belden CE, Hristov AD, Juraska JM (2013). Dendritic remodeling in the adolescent medial prefrontal cortex and the basolateral amygdala of male and female rats. Synapse 68(2): 61-72.

Krugers HJ, Arp JM, Xiong H, Kanatsou S, Lesuis SL, Korosi A, Joels M, Lucassen PJ (2017). Early life adversity: lasting consequences for emotional learning. Neurobiology of Stress 6: 14-21.

Lenroot RK, Gogtay N, Greenstein DK, Wells EM, Wallace GL, Clasen LS, Blumenthal JD, Lerch J, Zijdenbos AP, Evans AC, Thompson PM, Giedd JN (2007). Sexual dimorphism of brain developmental trajectories during childhood and adolescence. NeuroImage 36(4): 1065-1073.

Lenroot RK, Giedd JN (2010). Sex differences in the adolescent brain. Brain Cogn 72: 46-55.

Likhtik E, Paz R (2015). Amygdala-prefrontal interavtions in (mal)adaptive learning. Trends Neurosci 38(3): 158-166.

Lupien SJ, McEwan BS, Gunnar MR, Heim C (2009). Effects of stress throughout the lifespan on the brain, behaviour and cognition. Nature Reviews Neuroscience 10: 434-445.

Maccari S, Kruggers, HJ, Morley-Fletcher S, Szyf M, Brunton PJ (2014). The consequences of early-life adversity: neurobiological, behavioural and epigenetic adaptations. J Neuroendocrinol 26(10): 707-723.

Maroun M, Kavushansky A, Holmes A, Wellman C, Motanis H (2012). Enhanced extinction of aversive memories by high-frequency stimulation of the rat infralimbic cortex. PLoS ONE 7: e35853.

Martin L, Viljoen M, Kidd M, Seedat S (2014). Are childhood trauma exposures predictive of anxiety sensitivity in school attending youth? J Affect Disord 168: 5-12.

McEwen BS (2008). Understanding the potency of stressful early life experiences on brain body and function. Metabolism 57: s11-s15.

McGaugh JL (2004). The amygdala modulates the consolidations of memories of emotionally arousing experiences. Annu Rev Neurosci 27: 1-28.

Mennes M, Zuo XN, Kelly C, Di Martino A, Zang YF, Biswal B, Castellanos FX, Milham MP (2011). Linking inter-individual differences in neural activation and behavior to intrinsic brain dynamics. Neuroimage 54(4): 2950-2959.

Mouton PR, Gokhale AM, Ward NL, West MJ (2002). Stereological length estimation using spherical probes. Journal of Microscopy 206: 54-64.

Nephew BC, Huang W, Poirier GL, Payne GL, Jing JA (2017). Altered neural connectivity in adult female rats exposed to early life social stress. Behav Brain Res 316:225-233.

Nooner KB, Mennes M, Brown S, Castellanos FX, Leventhal B, Milham MP, Colcombe SJ (2013). Relationship of trauma symptoms to amygdala-based functional brain changes in adolescents. J Trauma Stress 26(6): 784-787.

Ono M, Kikusui T, Sasaki N, Ichikawa M, Mori Y, Murakami-Murofushi K (2008). Early weaning induces anxiety and precocious myelination in the anterior part of the basolateral amygdala of Balb/c mice. Neuroscience 156(4): 1103-1110.

Pattwell SS, Liston C, Jing D, Ninan I, Yang RR, Witztum J, Murdock MH, Dincheva I, Bath KG, Casey BJ, Deisseroth K, Lee FS (2016). Dynamic changes in neural circuitry during adolescence are associated with persistent attenuation of fear memories. Nature Communications 7: 11475.

Paxinos G, Watson C (1997). The rain brain in stereotaxic coordinates. Academic Press, New York.

Philip NS, Kuras YI, Valentine TR, Sweet LH, Tyrka AR, Price LH, Carpenter LL (2013). Regional homogeneity and resting state functional connectivity: Associations with exposure to early life stress. Psychiatry Research: Neuroimaging 214(3): 247-253.

Rakic P, Bourgeois JP, Goldman-Rakic PS (1994). Synaptic development of the cerebral cortex: implications for learning, memory, and mental illness. Progress in Brain Research 102: 227-243.

Riccomagno MM, Klodkin AL (2016). Sculpting neural circuits by axon and dendrite pruning. Annu Rev Cell Dev Biol 31: 779-805.

Schoenbaum G, Chiba AA, Gallagher M (2000). Changes in frunctional connectivity in orbitofrontal cortex and basolateral amygdala during learning and reversal training. J Neurosci 20(13): 5179-5189.

Selleck RA, Xhang W, Samberg HD, Padival M, Rosenkranz JA (2018). Limited prefrontal cortical regulation over the basolateral amygdala in adolescent rats. Sci Rep 8: 17171.

Senn V, Wolff SB, Herry C, Grenier F, Ehrlich I, Gründemann J, Fadok JP, Müller C, Letzkus JJ, Lüthi A (2014). Long-range connectivity defines behavioral specificity of amygdala neurons. Neuron 81(2): 428-437.

Smyke AT, Koga SF, Johnson DE, Fox NA, Marshall PJ, Nelson CA, Zeanah CH, BEIP Core Group (2007). The caregiving context in institution-reared and family-reared infants and toddlers in Romania. J Child Psychol Psychiatry 48(2): 210-218.

Spear LP (2000). The adolescent brain and age-related behavioral manifestations. Neurosci BiobehavRev 24(4): 417-463.

St Onge JR, Stopper CM, Zahm DS, Floresco SB (2012). Separate prefrontal-subcortical circuits mediate different components of risk-based decision making. J Neurosci 32(8): 2886-2899.

Swanson LW (2018). Brain maps 4.0-structure of the rat brain: an open access atlas with global nervous system nomenclature ontology and flatmaps. J Comp Neurol 526(6): 935-943.

Teicher MH, Samson JA, Anderson CM, Ohashi K (2016). The effects of childhood maltreatment on brain structure, function and connectivity. Nature Reviews Neuroscience 17: 652-666.

Thomason ME Dennis EL, Joshi AA, Joshi SH, Dinov ID, Chang C, Henry ML, Johnson RF, Thompson PM, Toga AW, Glover GH, Van Horn JD, Gotlib IH (2011a). Resting-state fMRI can reliably map neural networks in children. Neuroimage 55: 165-175.

Thomason ME, Hamilton JP, Gotlib IH (2011b). Stress-induced activation of the HPA axis predicts connectivity between subgenual cingulate and salience network during rest in adolescents. J Child Psychol Psychiatry 52(10): 1026-1034.

Thomason ME, Marusak HA, Tocco MA, Vila AM, McGarragle O, Rosenberg DR (2015). Altered amygdala connectivity in urban youth exposed to trauma. Social Cognitive and Affective Neuroscience 10(11): 1460-1468.

Tottenham N, Galván A (2016). Stress and the adolescent brain: amygdala-prefrontal cortex circuitry and ventral striatum as developmental targets. Neurosci Biobehav Rev 70: 217-227.

Tyrka AR, Burgers DE, Philip NS, Price LH, Carpenter LL (2013). The neurobiological correlates of childhood adversity and implications for treatment. *Acta Psychiatr Scand* 128(6): 434-447.

Tzanoulinou S, Sandi C (2016). The programming of the social brain by stress during childhood and adolescence: from rodents to humans. Social Behavior from Rodents to Humans. In Wöhr M, Krach S (eds) Social Behavior from Rodents to Humans. Current Topics in Behavioral Neurosciences, vol 30. Springer, Cham.

Van Eden CG, Uylings HB (1985). Cytoarchitectonic development of the prefrontal cortex in the rat. J Comp Neurol 241: 253-267.

Van Tieghem MR, Tottenham N (2018). Neurobiological programming of early life stress: functional development of amygdala-prefrontal circuitry and vulnerability for stress-related psychopathology. Curr Topics in Behav Neurosci 38: 117-136.

Wainwright NW, Surtees PG (2002). Childhood adversity, gender and depression over the life-course. J Affect Disord 72: 33-44.

Yang EJ, Lin EW, Hensch TK (2012). Critical period for acoustic preference in mice. Proc Natl Acad Sci USA 109: 17213-17220.

Zimmermann KS, Richardson R, Baker KD (2019). Maturational changes in prefrontal amygdala circuits in adolescence: implications for understanding fear inhibition during a vulnerable period of development. Brain Sci 9(3): E65.